Functional Signal Peptide Reduces Bilayer Thickness of Phosphatidylcholine Liposomes

Yoshikazu Tahara,*,‡ Masayuki Murata, and Shun-ichi Ohnishi

Department of Biophysics, Faculty of Science, Kyoto University, Kyoto 606, Japan

Yoshinori Fujiyoshi, Masakazu Kikuchi, and Yoshio Yamamoto§

Protein Engineering Research Institute, 6-2-3 Furuedai, Suita, Osaka 565, Japan

Received January 17, 1992; Revised Manuscript Received April 15, 1992

ABSTRACT: To investigate the interaction between a signal peptide and the lipid bilayer, two kinds of peptides, L8–M5 (L8 = $MRL_8PLAALG$, M5 = KVFER) and L14–M5 (L14 = $MRL_{14}PLAALG$), were examined in membranes composed of dioleoylphosphatidylcholine (DOPC). Peptides L8 and L14 are artificially designed signal sequences, and M5 is the N-terminal five residues of human lysozyme; L8 mediated effective secretion of human lysozyme in yeast, while L14 did not [Yamamoto, Y., et al. (1987) *Biochem. Biophys. Res. Commun. 149*, 431–436]. DOPC liposomes incorporating L8–M5 or L14–M5 were observed by electron cryomicroscopy as pairs of concentric circles, and the separation of the bilayer was measured along the membrane. Peptide L8–M5 was found to reduce the bilayer thickness, but L14–M5 did not. CD measurements revealed that L8–M5 adopted an α-helical conformation with random coil in the liposome membranes and that L14–M5 adopted a more helical and less random conformation than L8–M5. Fluorescence spectroscopy using both aqueous and membranous probes revealed that L8–M5 destabilized the lipid bilayer more strongly than L14–M5. These results suggest that functional L8–M5 reduces the bilayer thickness and destabilizes the lipid bilayer and that these activities are important for signal peptide function.

The most important role of the signal sequence in the process of protein secretion is to guide a nascent polypeptide chain from the cytoplasm, through the membrane of the endoplasmic reticulum (ER),[1] and into the lumen of the ER. Recently some of the proteins involved in secretion have been elucidated at the molecular level [for review, see Gierasch (1989) and Rapoport (1990)]. However, the detailed molecular mechanisms of the signal sequence interaction with the cell membrane are not yet completely understood.

It is well-known that there is no apparent homology among the primary structures of signal sequences; however, some common features can be found, such as the existence of a series of hydrophobic amino acids in the middle of the signal sequence (Watson, 1984). The highly hydrophobic nature of the signal peptide suggests that the signal sequence inserts into the ER membrane (von Heijne & Blomberg, 1979), and hydrophobic interactions are predicted to occur between the hydrophobic segment of the signal sequence and the hydrophobic region of the lipid bilayer. The conformations of the signal peptides of various proteins, therefore, have been intensively studied in highly hydrophobic environments: for example, the signal peptides of M13 coat protein (Shinnar & Kaiser, 1984), LamB (Briggs & Gierasch, 1984; Bruch et al., 1989), preimmunoglobulin L chain (Katakai & Iizuka, 1984), chicken lysozyme, and *Escherichia coli* proteins (Reddy & Nagaraj, 1989) have been studied using CD and NMR in membrane-like environments, such as aqueous trifluoroethanol (TFE), hexafluoroisopropyl alcohol, and detergent micelles. These studies revealed that the signal peptides adopt an α-helical conformation in highly hydrophobic environments. Moreover, this conformation has also been observed in the lipid monolayer using CD and FT-IR spectroscopies (Briggs et al., 1986; Batenberg et al., 1988b; Cornell et al., 1989). The α-helical conformation, however, shortens the length of the hydrophobic core of the signal peptides to about 20 Å, while the thickness of the hydrophobic region of the lipid bilayer is around 30 Å.

Recently, Yamamoto et al. (1987, 1989) have designed a series of simplified signal sequences and have shown that the signal sequence L8 (=$MRL_8PLAALG$) is highly functional but L14 (=$MRL_{14}PLAALG$) is not functional in the secretion of human lysozyme in yeast. The precursor human lysozyme with L14 was indeed synthesized in yeast cells, but it was not processed to the mature form (Yamamoto & Kikuchi, 1989). Translocation experiments using canine pancreas microsomes showed that this lysozyme precursor with L14 could not be translocated across the microsome membrane (Kohara et al., unpublished data). CD and NMR studies have indicated that L8 adopts an α-helical conformation in aqueous TFE, although its C-terminal region (PLAALG) is more flexible (Yamamoto et al., 1990). The length of the hydrophobic core of L8 is about 20 Å, assuming a completely α-helical structure (1.5 Å per residue in α-helix), which is shorter than the thickness of the hydrophobic region of the bilayer. If L14 adopts a similar conformation, its length would be 9 Å longer than that of L8, which is comparable to the thickness of the hydrophobic region of the bilayer. Therefore, the mode of interaction of the signal peptide with the bilayer might cope with mismatch

‡ Present address: Protein Engineering Research Institute, 6-2-3 Furuedai, Suita, Osaka 565, Japan.

§ Present address: Takeda Chemical Industries, Ltd., 2-17-85 Juso-Hommachi, Yodogawa-ku, Osaka 532, Japan.

[1] Abbreviations: ER, endoplasmic reticulum; CD, circular dichroism; TFE, trifluoroethanol; DOPC, dioleoylphosphatidylcholine; PPDPC, 1-palmitoyl-2-(pyrenedecanoyl)phosphatidylcholine; ANTS, 1-aminonaphthalene-3,5,8-trisulfonic acid; DPX, *N,N'*-xylylenebis(pyridinium bromide); TES, *N*-[tris(hydroxymethyl)methyl]-2-aminoethanesulfonic acid; PIPES, piperazine-*N,N'*-bis(2-ethanesulfonic acid); Tris, tris(hydroxymethyl)aminomethane.

0006-2960/92/0431-8747$03.00/0

between the length of its hydrophobic core and the thickness of the hydrophobic region of the lipid bilayer in a certain manner.

Killian et al. (1990a) demonstrated that the PhoE signal peptide induced the formation of a nonbilayer lipid structure. Tryptophan residues in signal peptides were also used to detect the hydrophobic interactions between signal peptides and lipids (Killian et al., 1990b; McKnight et al., 1991). However, the problem of the aforementioned length mismatch between the signal peptide and the bilayer remains.

A newly developed high-resolution electron cryomicroscope (Fujiyoshi et al., 1991) is a powerful tool for analyzing this problem. It has enabled us to directly observe the structures of frozen-hydrated materials, especially biological molecules (Fujiyoshi, 1989). Specimens for electron cryomicroscopy were prepared using the vitreous ice embedding method, which requires neither chemical fixation nor heavy-atom staining of the specimen and causes no structural changes in the component molecules (Taylor & Glaeser, 1974; Adrian et al., 1984). Lepault et al. (1985) have used the ice-embedding method to observe vitrified liposomes with an electron cryomicroscope and have demonstrated that the bilayer structure of the liposome is resolved in such an image. Thus, the application of this method makes it possible to detect the changes in the thickness of the bilayer caused by signal peptides.

In the present study, we examined the interactions of functional (L8) and nonfunctional (L14) signal peptides with the lipid bilayer of phosphatidylcholine liposomes, using the electron cryomicroscope as well as CD and fluorescence spectroscopies. Our results indicate that L8, but not L14, reduces the bilayer thickness and perturbs the integrity of lipid membranes.

MATERIALS AND METHODS

Materials. 1,2-Dioleoylphosphatidylcholine (DOPC) was purchased from Avanti Polar Lipids. 1-Palmitoyl-2-(pyrenedecanoyl)phosphatidylcholine (PPDPC) was a gift from Dr. Kinnunen. 1-Aminonaphthalene-3,6,8-trisulfonic acid (ANTS) and *N,N'*-xylylenebis(pyridinium bromide) (DPX) were purchased from Molecular Probes, and fluorescamine was obtained from Ciba-Geigy. Peptides were synthesized by the solid-phase method (Yamamoto et al., 1990).

Preparation of Peptide-Including Liposomes. Liposomes made of DOPC and L8–M5 (=MRL_8PLAALG–KVFER) or L14–M5 (=MRL_{14}PLAALG–KVFER) were prepared as follows: DOPC dissolved in chloroform was mixed with the peptide in chloroform–methanol (2:1 in volume) so that molar ratios of peptide to lipid were 0, 1/10, and 1/60. These solutions were dried in glass test tubes, and the organic solvent was thoroughly removed in vacuo for several hours. TES buffer (145 mM NaCl, 5 mM TES–NaOH, pH 7.4) was added to the peptide–lipid mixtures to yield a lipid concentration of about 10 mM. The mixtures were sonicated on ice, using a probe-type sonicator under a nitrogen atmosphere, until the suspension became clear.

Electron Cryomicroscopy. The liposomes were observed by electron cryomicroscopy combined with the vitreous ice-embedding technique developed by Adrian et al. (1984). The liposome suspension (2–4 μL) was applied to an EM grid supporting a gold-coated microgrid, which was glow discharged just before use. As soon as most of the suspension was removed with a small piece of filter paper, the EM grid was plunged into liquefied ethane (at about 100 K) to embed the liposomes in the vitreous ice film. The grid was transferred into the newly designed electron cryomicroscope (Fujiyoshi et al., 1991) with the specimen kept below 130 K with liquid nitrogen so as to prevent devitrification of the ice. The specimen was observed at a stage temperature of 4 K and an accelerating voltage of 400 kV. Electron micrographs were taken at ×40 000 magnification with an illuminating electron dose of approximately 80 e/Å^2 on the specimen plane.

CD Measurements. Liposomes were prepared as described above at a lipid concentration of 1 or 2 mM to minimize the effect of light scattering. CD spectra of liposomes were measured in a 1 mm thick quartz cell with a JASCO J-600 spectropolarimeter.

Peptide Association with Liposomes. Association of the peptides with the liposomes was monitored as described by Shen et al. (1982). A suspension (50 μL) of liposomes prepared for electron microscopy was mixed with 50 μL of PIPES buffer (130 mM NaCl, 20 mM PIPES–NaOH, pH 7.4) for centrifugation on a Ficoll (Pharmacia) density gradient. The suspension (100 μL) was mixed with the same volume of a PIPES-buffered 25% Ficoll solution, yielding a final concentration of 12.5% Ficoll. This suspension was overlaid successively by 1 mL of a PIPES-buffered 10% Ficoll solution and by 1 mL of PIPES buffer without Ficoll and then centrifuged at 3700*g* for 30 min. After centrifugation, the gradient was fractionated into 100-μL portions from bottom to top, and the vesicle concentration in each fraction was estimated by measuring the 90° light scattering. Most of the vesicles were concentrated at the interface between the 10% Ficoll step and the buffer solution. The peptide concentration was determined by fluorescamine assay.

Preparation of ANTS–DPX-Encapsulating Liposomes. Liposomes containing an ANTS–DPX complex were prepared by the reversed-phase evaporation method of Szoka and Papahadjopoulos (1978) with slight modifications. Dried DOPC (5 μmol) was dissolved with 3 mL of diethyl ether in a round-bottom flask and was then added to 1 mL of ANTS–DPX solution (12.5 mM ANTS, 45 mM DPX, 20 mM NaCl, 10 mM Tris-HCl, pH 7.4) prepared according to the method of Ellens et al. (1985). The sonicated mixture was placed on a rotary evaporator, and the diethyl ether was removed at 20 °C. An additional 1 mL of the ANTS–DPX solution was mixed with this suspension, which was incubated in a water bath at 40–50 °C for 1 h to completely remove the organic solvent. Free ANTS and DPX were removed from the liposomes by Ficoll density-gradient centrifugation (see Peptide Association with Liposomes). The liposomes were focused at the interface between the 10% Ficoll step and the buffer solution, while the free ANTS and DPX were trapped in the 12.5% Ficoll solution. The liposomes were collected and diluted with PIPES buffer to yield a lipid concentration of 5 mM.

Leakage Measurement of ANTS–DPX Complex. Leakage of the ANTS–DPX complex from the liposomes was monitored with a Hitachi 850S fluorescence spectrometer. The liposome suspension (50 μL) was diluted with 500 μL of PIPES buffer in a square quartz microcell, and the peptide, dissolved in TFE (5 mM), was added to the suspension. The peptide concentration was 133 μM. The increase in ANTS fluorescence intensity was monitored at 531 nm using an excitation wavelength of 384 nm for 5 min. The 100 and 0% leakage values were taken as the fluorescence intensities of the liposome suspension after the additions of 0.3% Triton X-100 and TFE, respectively.

Measurement of Pyrene Excimer Formation in the Hydrophobic Region of the Lipid Bilayer. A liposome suspension

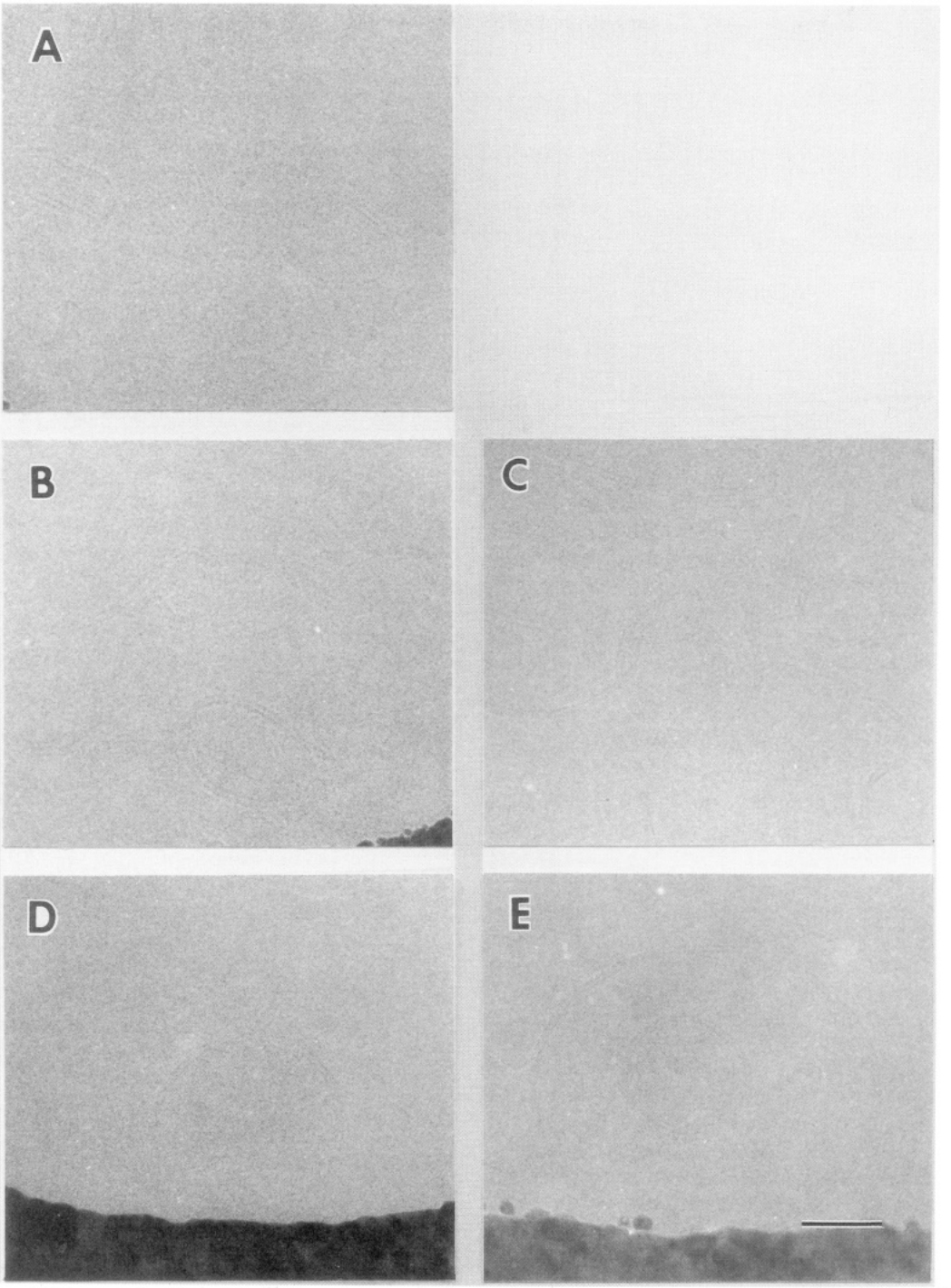

FIGURE 1: Images of liposomes in vitreous ice. Liposomes were made of (A) DOPC only (P/L = 0), (B) DOPC and L8–M5 (P/L = 1/60), (C) DOPC and L8–M5 (P/L = 1/10), (D) DOPC and L14–M5 (P/L = 1/60), and (E) DOPC and L14–M5 (P/L = 1/10). The bar indicates 500 Å. The shadow-like images in the photographs (B, D, E) are microgrid frames. The separation of the bilayer image (referred to as the peak separation) was measured along the bilayer of each liposome image.

was prepared from a lipid mixture of DOPC and PPDPC (in a molar ratio of 4/1) by sonication. Five minutes after the peptide (dissolved in TFE) was added to the liposome suspension, the fluorescence spectrum of pyrene was measured with a Hitachi 850S fluorescence spectrometer, using an excitation wavelength of 350 nm.

Simulation of the Bilayer Image. A liposome embedded in vitreous ice was observed as a pair of concentric circles, the separation of which varied widely. To explain this variation, a simulation of a bilayer image was created using the MULTI SLICE program of Ishizuka and Uyeda (1977), which is based on a simple model: it is constructed using only the headgroups of the lipid molecules (for details, see the legend of Figure 7). All of the parameters involved in the image simulation were the same as those in the real observation. The liposome diameter was fixed to 1000 Å, and there was no dependence of the simulated bilayer thickness on the diameter from 200 to 2000 Å.

RESULTS

Electron Cryomicroscopy of Liposomes. Five kinds of liposomes were prepared: DOPC only, DOPC with L8–M5 at the two peptide–lipid molar ratios (P/L) of 1/60 and 1/10, and DOPC with L14–M5 at the same two P/Ls. All five preparations were observed with the electron cryomicroscope.

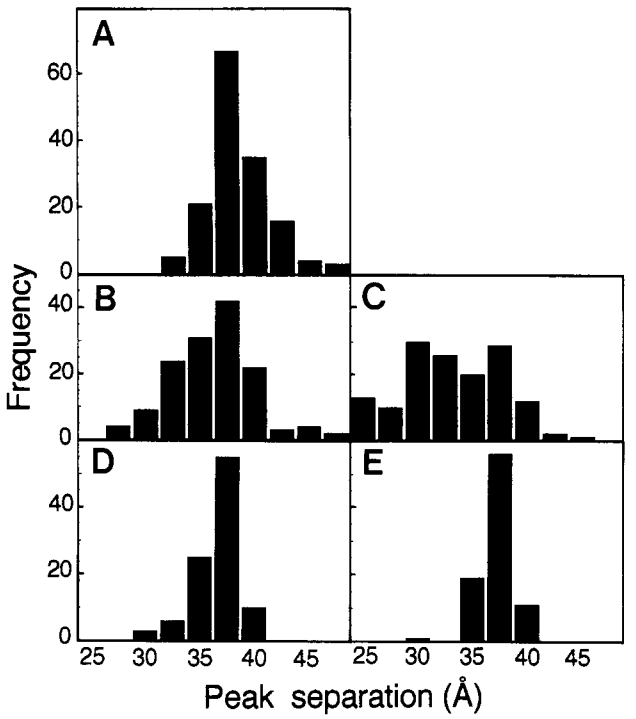

FIGURE 2: Distributions of the peak separations illustrated as histograms. (A) DOPC liposome (P/L = 0); (B) DOPC–L8–M5 liposome (P/L = 1/60); (C) DOPC–L8–M5 liposome (P/L = 1/10); (D) DOPC–L14–M5 liposome (P/L = 1/60); (E) DOPC–L14–M5 liposome (P/L = 1/10).

In each instance the liposomes appeared as pairs of concentric circles, as shown in Figure 1. The separation of these two density peaks (referred to as the "peak separation") was measured perpendicularly to the circumference of the liposome every 12.5 Å along the bilayer image. The measurement results are summarized as histograms (Figure 2). The maximum, minimum, and mean values of the peak separations are given in Table I. These results indicate that the mean peak separation, d_{mean}, of the L8–M5–DOPC liposomes was reduced but that of the L14–M5–DOPC liposomes was less significantly affected.

The measurement results are summarized as follows: (1) The peak separations of the images of all five types of liposomes varied widely. (2) L8–M5 significantly reduced the mean peak separation, while L14–M5 did so only marginally. (3) The reduction of the mean peak separation caused by L8–M5 was increased with an increase of P/L. (4) In the case of the L8–M5–DOPC liposome, the distribution of the peak separation was more widespread than that of DOPC liposome. (5) The L14–M5–DOPC liposome had a narrower distribution of peak separation than the DOPC liposome.

Estimation of the Secondary Structures of the Peptides Based on the CD Spectra. The CD spectrum of each peptide was measured in two different sets of environments (Figure 3), aqueous TFE [100, 50, and 20%; (A) for L8–M5 and (B) for L14–M5] and DOPC liposomes [P/L = 1/100, 1/60, and 1/10; (C) for L8–M5 and (D) for L14–M5]. We calculated the percentage of α-helical content of the peptide in each environment from the equation

$$\% \ \alpha\text{-helix} = ([\theta]_{208nm} - 4000)/(33000 - 4000)$$

which was presented in Greenfield and Fasman (1969). The results are summarized in Table II.

Association of Peptides with the Liposome Membrane. Discontinuous Ficoll density gradient assays were performed to measure the association of the peptides with the membranes of liposomes used for electron cryomicroscopy and CD measurement. The liposomes float to the upper fractions (fractions 5 and 6 in Figure 4) of the gradient, while free peptides or peptide micelles remain at the bottom. When the peptide without liposomes was applied to the gradient, it remained in the bottom fraction after centrifugation (data not shown). In the presence of liposomes, however, the peptides comigrated with the liposomes to the upper fractions as expected, suggesting that the peptide associated with the liposomes under these experimental conditions.

Peptide-Induced Leakage of ANTS–DPX Complex from Liposomes. ANTS is quenched by encapsulation with an excess of DPX in liposomes but becomes fluorescent by dilution of the DPX when the ANTS–DPX complex leaks from the liposomes (Ellens et al., 1985). Thus, the leakage of the liposome contents can be detected by measurement of the increase in ANTS fluorescence. Both peptides released the encapsulated ANTS–DPX complex, but L8–M5 caused greater leakage of the contents than L14–M5 at each peptide concentration, throughout all of the measurements (Figure 5).

Peptide Inhibition of Pyrene Excimer Formation in the Lipid Membranes. Fluorescence spectra of PPDPC were measured 5 min after the peptide solution in TFE was added to the liposome suspension. The peptide concentrations were 23, 27, 36, and 45 μM. Typical changes in the fluorescence spectra by the addition of L8–M5, of L14–M5 at P/L = 1/10, and of TFE (control) are shown in Figure 6A. Characteristic peaks were observed at 370 and 470 nm, which were derived from excited pyrene monomers and excimers, respectively, where the excimer was formed by the collision of an excited pyrene and a ground-state pyrene. The ratio of fluorescence from the excimer to that of the monomer, I_E/I_M, consequently represents the environmental change around the pyrene molecules in the hydrophobic region of the lipid bilayer (Kinnunen et al., 1987). The degree of inhibition of excimer formation by L8–M5 and L14–M5 is also shown in Figure 6B, indicating that a larger P/L caused a higher degree of inhibition of excimer formation. It is also shown that the inhibition by L8–M5 was stronger than that by L14–M5.

Simulation of Bilayer Images. The bilayer image was simulated to estimate the area of the "thickness-reduced zone" according to the series of simple models of liposomes (for example, Figure 7B). One of the simulated density profiles of the bilayer images is shown in Figure 7C. The two peaks correspond to the densities derived from the two arrays of phosphorus atoms, that is, the two leaflets of the membrane. The result of the image simulation can be summarized as follows: when the height of the thickness-reduced zone (W) is more than 100 Å, the image of the bilayer becomes thinner (Figure 7D).

DISCUSSION

Electron Cryomicroscopy. Many physicochemical studies of the interactions between natural or synthetic signal peptides and the lipid bilayer of liposomes have been carried out. Batenburg et al. (1988a) and Killian et al. (1990a) showed by freeze–fracture electron microscopy that integration of the signal peptide induced a morphological change in the liposome membranes that cannot be directly investigated by other physicochemical means.

Recently, we have developed a new method to measure the thickness of the lipid bilayer of liposomes by combining the ice-embedding method with electron cryomicroscopy. This technique enabled us to find not only an irregularity in the

Table I: Results of the Peak Separation Measurements (All Values Were Calculated Using Three Liposome Preparations for Each Specimen)

specimen	P/L	peak separations (Å)			relation between peak separations (Å)	
		d_{max}	d_{min}	d_{mean} (SD[a])	$d_{max} - d_{min}$	Δd_{mean}
DOPC liposome	0	47.5	32.5	38.5 (2.9)	15.0	
L8–M5–DOPC liposome	1/60	47.5	27.5	36.2 (3.9)	20.0	2.3
	1/10	45.0	25.0	33.2 (4.6)	20.0	5.3
L14–M5–DOPC liposome	1/60	40.0	30.0	36.6 (2.2)	10.0	1.9
	1/10	40.0	30.0	37.2 (1.7)	10.0	1.3

[a] Standard deviation.

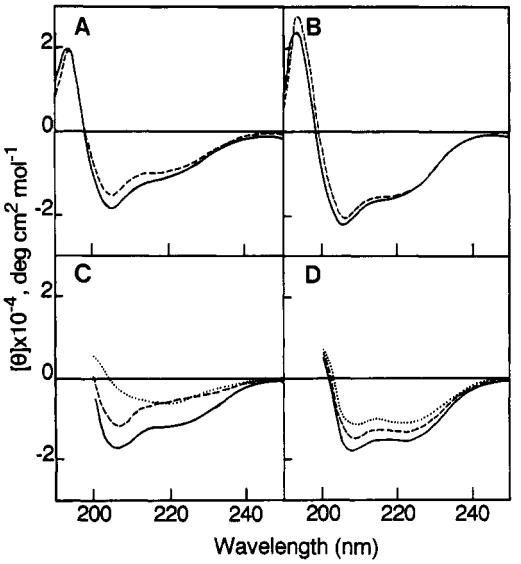

FIGURE 3: CD spectra of L8–M5 and L14–M5 in two different environments. One is aqueous TFE [(A) L8–M5 (B) L14–M5], and the other is phosphatidylcholine membranes [(C) L8–M5 (D) L14–M5]. In (A) and (B), the solid lines indicate the spectra in 100% TFE and the broken lines denote the spectra in 20% TFE. The spectra of both peptides in 50% TFE are omitted because they are essentially identical to those in 100% TFE. In (C) and (D), the peptide–lipid ratios (P/L) vary as follows: P/L = 1/100 (solid lines), P/L = 1/60 (broken lines), and P/L = 1/10 (dotted lines). The spectra below 200 nm for the liposome membranes cannot be shown because of the high noise level.

Table II: Percentages of α-Helix Content of the Peptides in Aqueous TFE and in Liposome Membranes

environment	L8–M5		L14–M5	
	α	remainder[a]	α	remainder
aqueous TFE				
100%	51	49	63	37
50%	48	52	63	37
20%	40	60	58	42
liposome membrane				
P/L = 1/100	46	54	49	51
P/L = 1/60	31	69	38	62
P/L = 1/10	0	100	26	74

[a] β-structure and random coil.

thickness of the lipid bilayer of the liposomes but also a thickness change due to differences in the acyl chain species of the lipid molecule (Tahara and Fujiyoshi, unpublished results). We therefore applied this new method to the model membranes, composed of signal peptides and DOPC liposomes, to elucidate the interaction between the hydrophobic region of the signal peptide and that of the lipid bilayer.

We have measured the peak separations of the bilayer image of each liposome image, and the results are summarized in the previous section and Table I. The error of observation was calculated to be within ±0.7 Å, which was determined from the lattice images of chlorinated copper phthalocyanine: this

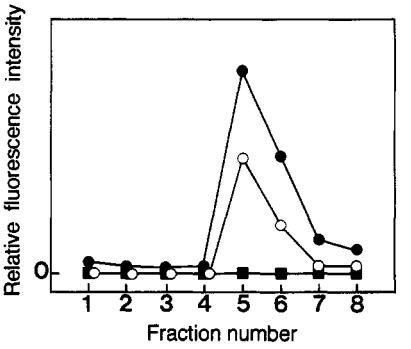

FIGURE 4: Association of peptide with liposomes measured by fluorescamine, which is fluorescent only when bound to the NH_3^+ groups of the peptide. The fluorescence intensities for L8–M5 (○), L14–M5 (●), and DOPC liposomes (■) are plotted against the fraction number (see Materials and Methods for details). The liposome-containing fraction was identified as the fifth fraction by the measurement of scattered-light (wavelength of 400 nm) intensity to the 90° direction (data not shown).

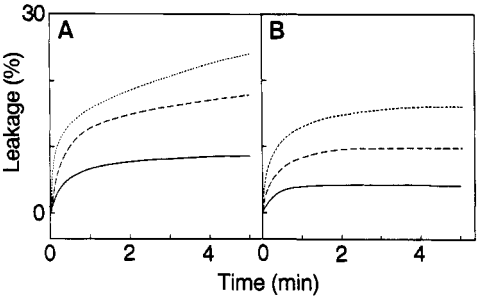

FIGURE 5: ANTS–DPX complex, encapsulated in DOPC liposomes, released by (A) L8–M5 and (B) L14–M5 and monitored by an excitation wavelength of 390 nm and an emission wavelength of 475 nm. The peptide concentrations were 45 (solid lines), 89 (broken lines), and 133 μM (dotted lines).

error value enhances the reliability of our measurements. The result (1) implies an irregularity in the membrane structure of the DOPC liposome, a phenomenon which has also been observed in liposomes composed of other kinds of phosphatidylcholines (Tahara and Fujiyoshi, unpublished results). The results (2) and (3) suggest that L8–M5 caused a thickness reduction of the hydrophobic region of the lipid bilayer. Since at P/L = 1/60, the Δd_{mean} = 2.3 Å is less than the standard deviation (SD) of 3.9 Å (Table I), the reduction of the bilayer thickness is not apparent. At P/L = 1/10, the Δd_{mean} (5.3 Å) is larger than the SD (4.6 Å); therefore, the peak separation was apparently reduced. This reduction can be explained by the fact that L8 is shorter than the thickness of the hydrophobic region of the lipid bilayer. By contrast, L14–M5 caused only a slight reduction of the separation of the bilayer, as compared to L8–M5: at both P/Ls, the Δd_{mean} values (1.9 and 1.3 Å) are smaller than the SDs (2.2 and 1.9 Å, respectively). This is probably because the length of L14 is nearly equal to the thickness of the hydrophobic region of the lipid bilayer.

Although the variation of the d values ($d_{max} - d_{min}$) in the L8–M5–DOPC liposome was equal at P/L = 1/60 and 1/10

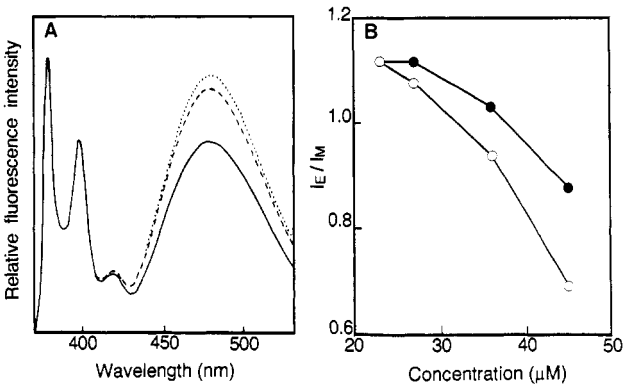

FIGURE 6: Inhibition of pyrene excimer formation in liposome membranes by L8–M5 and L14–M5. PPDPC is fluorescent at 370 (due to monomer) and 470 nm (due to excimer). (A) Fluorescence spectra of DOPC liposomes incorporating PPDPC measured after mixing 45 μM L8–M5 (solid line) or L14–M5 (broken line). The dotted line shows the spectrum of liposomes without peptide. The spectra were normalized by the fluorescent intensity of the monomer, I_M. (B) Concentration dependence of the intensity ratio of excimer to monomer, I_E/I_M: (○) L8–M5; (●) L14–M5.

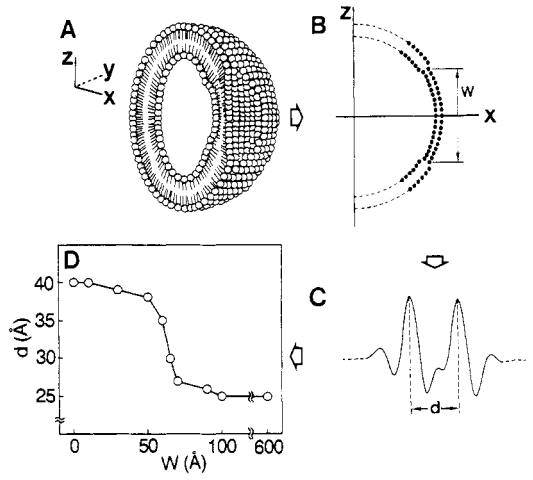

FIGURE 7: Procedure of image simulation of the lipid bilayer using the MULTI SLICE program. (A) Diagram of a section of a liposome with an area where the bilayer is thinned (referred to as the thickness-reduced zone). The inset represents the x,y,z axes, corresponding to both the diagram and the z,x axes in the view from the y direction of this diagram (B). Since the viewing direction by the electron microscope is parallel to the z direction, the simulated image is projected on the x,y plane. The two arrays of dots represent phosphorus atoms in the headgroups of the lipid molecules. The separation between the two arrays of phosphorus atoms, that is, the bilayer thickness, was set to 40 Å as a normal thickness. In the thickness-reduced zone, the bilayer was thinned to 25 Å and its height, W, was varied from 0 to 600 Å. (C) One of the intensity profiles of the simulated bilayer image along the x direction. The two main peaks correspond to the density of the bilayer, and d represents the peak separation of the simulated bilayer image. (D) Simulated peak separation as a function of W.

(Table I), the d_{mean} was smaller at P/L = 1/10 than at P/L = 1/60. As revealed by the image simulation (Figure 7), significant bilayer thinning requires a height larger than 100 Å for the thickness-reduced zone. Therefore, there are either more or larger sizes of the thickness-reduced zones at P/L = 1/10 than at P/L = 1/60. The peptide L14–M5, on the other hand, did not reduce the bilayer thickness, but the standard deviations were smaller, probably because the length of the hydrophobic core of the peptide is the same as the thickness of the hydrophobic region of the bilayer. This may diminish the irregularity in the membrane.

Conformation of Peptide in the Lipid Bilayer. As Figure 3 and Table II indicate, the conformations of L8–M5 and L14–M5 in aqueous TFE remained essentially unchanged with variation of the TFE concentration. On the other hand, in the liposome membranes, the conformations of both peptides changed markedly according to the peptide–lipid ratio (P/L). In fact, the conformation of L8–M5 at P/L = 1/100 was almost the same as that in aqueous TFE, but the α-helical content was 0% at P/L = 1/10 (Table II), which would make the peptide longer than at smaller P/Ls. This may seem to be in conflict with the results that higher concentrations of the peptide tend to thin the liposome membranes. However, either adsorption of the peptide to the lipid membrane (Cornell et al., 1989) or aggregation of the peptides in the membrane can induce β-structure, resulting in a decrease in the α-helical conformation. Moreover, as shown by Mao and Wallace (1984), the large size of the membrane particles and the high local concentration of the proteins in these particles distort the CD spectra of membrane proteins and produce erroneous estimates of the secondary structure. There are two points that are relevant to the conditions of L8–M5 in the liposome membranes at P/L = 1/10: large liposomes remained in the specimen after thorough sonication (data not shown), and the peptides were highly condensed on the membranes. Although we could find images of relatively small liposomes among the various sizes of liposome images when we measured the bilayer thickness, the CD measurements may have been strongly affected by the larger membrane moieties. They may have veiled the signals from the peptides in small vesicles, which would have indicated the correct α-helical conformation. All of the possibilities described above might contribute to the lack of α-helical content of L8–M5 at P/L = 1/10. Therefore, it is reasonable to conclude that the CD measurement at the lowest P/L, 1/100, where the peptide conformation is almost the same as that in aqueous TFE, is more appropriate for discussion of the secondary structure than the measurement at the higher P/L.

The conformation of L8 in aqueous TFE proved to be highly α-helical and its C-terminal region (PLAALG) dynamically changed to a less helical conformation by thermal vibration (Yamamoto et al., 1990). According to this conformational alteration, the length of the hydrophobic core of L8 varies between 21 (completely helical, 1.5 Å × 14) and 34 Å (with PLAALG extended, 1.5 Å × 8 + 3.6 Å × 6). The length variation of the hydrophobic core of L8 is consistent with the thickness variation of the hydrophobic region of the membrane composed of DOPC and L8–M5. This was calculated to be about 20–35 Å by considering that the spacing between the phosphorus atom in the lipid headgroup and the first carbon atom of the acyl chain is about 5 Å (Pearson & Pasher, 1979). In the case of L14, the length of the hydrophobic core of 20 residues, L_{14}PLAALG, was calculated to be from 30 (completely helical, 1.5 Å × 20) to 43 Å (with PLAALG extended, 1.5 Å × 14 + 3.6 Å × 6) when the same conformation as L8–M5 is assumed. This partly extended hydrophobic core, which is about 5 Å longer than the maximum thickness of the hydrophobic region of the DOPC membrane, would thicken the lipid bilayer. However, the measured bilayer thickness of the L14–M5–DOPC liposome is less than 40 Å, and therefore, the extended PLAALG region may not affect the structure of the bilayer.

Destabilization of the Lipid Bilayer by the Peptides. The differences in the interactions of L8–M5 and L14–M5 with the lipid bilayer were examined by fluorescence measurements. By monitoring fluorophore release from liposomes, Roise et al. (1988) showed that a functional presequence of a mitochondrial protein disrupted phospholipid vesicles. Peptides

L8–M5 and L14–M5 both allowed leakage of ANTS–DPX from the inside of the liposomes, but L8–M5 released the liposome content to a greater extent than L14–M5 (Figure 5). Interestingly, L8–M5 caused lipid mixing between the liposomes but L14–M5 did not, as revealed by the resonance energy transfer between the two different membranous fluorophores (data not shown) according to the method of Murata et al. (1992). Although we cannot determine whether the lipid mixing was caused by liposome fusion or by tight aggregation of liposomes, we can conclude that L8–M5 modulates the phospholipid bilayer more strongly than L14–M5, and this correlates with the difference between these two peptides in their abilities to support secretion.

Effect of the Peptides on Lipid Lateral Diffusion. PPDPC is a membranous fluorescent probe that allows monitoring of changes in its lateral mobility in the lipid bilayer. The ratio of the fluorescence intensity of a pyrene excimer and that of a pyrene monomer, I_E/I_M, is reduced when the collision probability of pyrenes decreases (Kinnunen et al., 1987). Therefore, the peptide-induced reduction of I_E/I_M is attributed to the effect of the peptides reducing the collision probability of pyrene in the membrane. There are two explanations for this phenomenon. First, the peptides inserted into the membrane lower the concentration of pyrene in the membrane; if this was the only explanation, then L8–M5 and L14–M5 would display the same effect on pyrene excimer formation. Second, the interaction between the hydrophobic segment of the peptide and the hydrophobic acyl chains of lipids reduces the lateral diffusion rate of the pyrene or causes a lateral phase separation of the lipids. The results support the second reason: L8–M5 yields lower I_E/I_M values than L14–M5 at every peptide concentration measured except the lowest (Figure 6). L8–M5 may interact with PPDPC more strongly than L14–M5 in the lipid bilayer. This result suggests that L8–M5 binds the surrounding lipid molecules and reduces the movement of the lipid; as a result, pyrene excimer formation is diminished. This interpretation is supported by the results of electron cryomicroscopy and image simulation: the reduction of the peak separation of the bilayer image requires a relatively large domain where the bilayer thickness is reduced (Figure 7D). The lipid molecules are probably bound tightly to the peptides that penetrate the lipid bilayer and induce the phase separation between this thickness-reduced zone and the bulk lipid molecules.

Mechanism of Bilayer Thickness Reduction. Finally, we would like to discuss the mechanism of the bilayer thickness reduction induced by L8–M5 but not significantly by L14–M5. As mentioned above, there is a difference in the length of the hydrophobic core of L8 and the thickness of the hydrophobic region of the lipid bilayer. If L8–M5 did not cause a reduction of the bilayer thickness, the acyl chains of the lipids around the peptide would be exposed to a hydrophilic environment. The hydration of alkane is highly unstable because of a loss of free energy (Ooi et al., 1987). Moreover, there would be a repulsive interaction between the polar amino acid residues and the hydrophobic acyl chains of the lipids surrounding the peptide (Figure 8A); this would cause a further loss of free energy. The structure of the lipids around L8–M5 would therefore be more stable in the form illustrated in Figure 8B, which gives further support for the "mattress model" (Mouritsen & Bloom, 1984). This structure may give rise to a zone in which the separation between the polar headgroups across the membrane is smaller than in the other areas, and the lipid molecules become unstable from the standpoint of the free energy (Mouritsen & Bloom, 1984). To lower the loss of free energy due to the perturbation, the peptides may aggregate in the membrane, because the aggregation of the peptides makes the distorted area smaller. Lewis and Engelman (1983) have already pointed out that this kind of aggregation is promoted by a mismatch between the length of the hydrophobic core of the peptide and the thickness of the hydrophobic regionof the lipid bilayer. Since the length of L14 is similar to the thickness of the hydrophobic region of the lipid bilayer (Figure 8C), L14–M5 does not perturb the lipid bilayer as much as L8–M5. This discussion is also consistent with the differences in the extent of the liposome leakage and the inhibition of the pyrene excimer formation, because a greater interaction between the peptide and the lipid causes a larger disturbance in the liposome membrane.

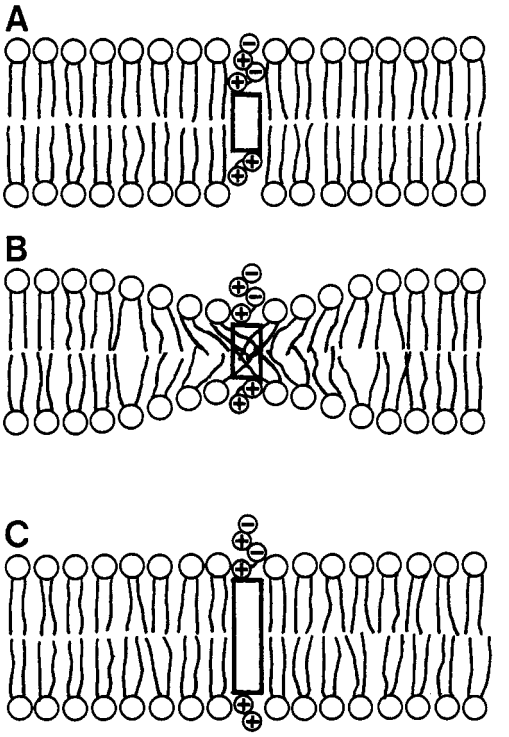

FIGURE 8: Models of L8–M5 (A, B) and L14–M5 (C) in the lipid bilayer. Each lipid is drawn as a circle with a pair of curved lines, indicating a head group and acyl chains, respectively, and a peptide is represented as a rectangle and circled plus or minus symbols, indicating the hydrophobic segment and the charged amino acids [for example, in L8–M5, NH_3^+ of Met^1, $(Arg^2)^+$, $(Lys^{17})^+$, $(Glu^{20})^-$, $(Arg^{21})^+$, and COO^- of (Arg^{21})]. (A) Possible interference between the hydrophobic acyl chains and the charged amino acids, if the thickness of the membranes was not reduced. (B) Model of the lipid configuration around the peptide. Reduction of the thickness of the lipid bilayer can avoid such interference, as illustrated in (A). The hydrophobic segment of L14–M5 is long enough to maintain the bilayer thickness (C).

In conclusion, L8, the potent signal sequence, was found to be physically "active" in the lipid bilayer through its interaction with lipid molecules. This activity subsequently causes a change in the structure of the lipid bilayer, a reduction of the bilayer thickness, and a destabilization of the bilayer structure, which cause the membrane to become more permeable and possibly help the translocation of a secretory protein across the ER membrane.

ACKNOWLEDGMENT

We thank Drs. Tatsuo Miyazawa and Peter Tulloch for critically reading the manuscript and Dr. Kosuke Morikawa and Mr. Koji Inaka for discussions and suggestions.

REFERENCES

Adrian, M., Dubochet, J., Lepault, J., & McDowall, A. W. (1984) *Nature 308*, 32–36.

Batenburg, A. M., Demel, R. A., Verkleij, A. J., & de Kruijff, B. (1988a) *Biochemistry 27*, 5678–5685.

Batenburg, A. M., Brasseur, R., Ruysschaert, J.-M., van Scharrenburg, G. J. M., Slotboom, A. J., Demel, R. A., & de Kruijff, B. (1988b) *J. Biol. Chem. 263*, 4202–4207.

Briggs, M. S., & Gierasch, L. M. (1984) *Biochemistry 23*, 3111–3114.

Briggs, M. S., Cornell, D. G., Dluhy, R. A., & Gierasch, L. M. (1986) *Science 233*, 206–208.

Bruch, M. D., McKnight, C. J., & Gierasch, L. M. (1989) *Biochemistry 28*, 8554–8561.

Cornell, D. G., Dluhy, R. A., Briggs, M. S., McKnight, C. J., & Gierasch, L. M. (1989) *Biochemistry 28*, 2789–2797.

Ellens, H., Bentz, J., & Szoka, F. C. (1985) *Biochemistry 24*, 3099–3106.

Fujiyoshi, Y. (1989) *J. Electron Microsc. 38*, S97–S101.

Fujiyoshi, Y., Mizusaki, T., Morikawa, K., Yamagishi, H., Aoki, Y., Kihara, H., & Harada, Y. (1991) *Ultramicroscopy 38*, 241–251.

Gierasch, L. M. (1989) *Biochemistry 28*, 923–930.

Greenfield, N., & Fasman, G. D. (1969) *Biochemistry 8*, 4108–4116.

Ishizuka, K., & Uyeda, N. (1977) *Acta Crystallogr. A33*, 740–749.

Katakai, R., & Iizuka, Y. (1984) *J. Am. Chem. Soc. 106*, 5715–5718.

Killian, J. A., de Jong, A. M. Ph., Bijvelt, J., Verkleij, A. J., & de Kruijff, B. (1990a) *EMBO J. 9*, 815–819.

Killian, J. A., Keller, R. C. A., Struyvé, M., de Kroon, A. I. P. M., Tommassen, J., & de Kruijff, B. (1990b) *Biochemistry 29*, 8131–8137.

Kinnunen, P. K. J., Tulkki, A.-P., Lemmetyinen, H., Paakkola, J., & Virtanen, J. A. (1987) *Chem. Phys. Lett. 136*, 539–545.

Lepault, J., Pattus, F., & Martin, N. (1985) *Biochim. Biophys. Acta 820*, 315–318.

Lewis, B. A., & Engelman, D. M. (1983) *J. Mol. Biol. 166*, 203–210.

Mao, D., & Wallace, B. A. (1984) *Biochemistry 23*, 2667–2673.

McKnight, C. J., Rafalski, M., & Gierasch, L. M. (1991) *Biochemistry 30*, 6241–6246.

Mouritsen, O. G., & Bloom, M. (1984) *Biophys. J. 46*, 141–153.

Murata, M., Takahashi, S., Kagiwada, S., Suzuki, A., & Ohnishi, S. (1992) *Biochemistry 31*, 1986–1992.

Ooi, T., Oobatake, M., Némethy, G., & Scheraga, H. A. (1987) *Proc. Natl. Acad. Sci. U.S.A. 84*, 3086–3090.

Pearson, R. H., & Pascher, I. (1979) *Nature 281*, 499–501.

Rapoport, T. A. (1990) *Trends Biol. Sci. 15*, 355–358.

Reddy, G. L., & Nagaraj, R. (1989) *J. Biol. Chem. 264*, 16591–16597.

Roise, D., Theiler, F., Horvath, S. J., Tomich, J. M., Richards, J. H., Allison, D. S., & Schatz, G. (1988) *EMBO J. 7*, 649–653.

Shen, de-F., Huang, A., & Huang, L. (1982) *Biochim. Biophys. Acta 689*, 31–37.

Shinnar, A. E., & Kaiser, E. T. (1984) *J. Am. Chem. Soc. 106*, 5006–5007.

Szoka, F., Jr., & Papahadjopoulos, D. (1978) *Proc. Natl. Acad. Sci. U.S.A. 75*, 4194–4198.

Taylor, K. A., & Glaeser, R. M. (1974) *Science 186*, 1036–1037.

von Heijne, G., & Blomberg, C. (1979) *Eur. J. Biochem. 97*, 175–181.

Watson, M. E. E. (1984) *Nucleic Acids Res. 13*, 5145–5164.

Yamamoto, Y., & Kikuchi, M. (1989) *Eur. J. Biochem. 187*, 233–236.

Yamamoto, Y., Taniyama, Y., Kikuchi, M., & Ikehara, M. (1987) *Biochem. Biophys. Res. Commun. 149*, 431–436.

Yamamoto, Y., Taniyama, Y., & Kikuchi, M. (1989) *Biochemistry 28*, 2728–2732.

Yamamoto, Y., Ohkubo, T., Kohara, A., Tanaka, T., Tanaka, T., & Kikuchi, M. (1990) *Biochemistry 29*, 8998–9006.

Registry No. L8-M5, 129149-12-8; L14-M5, 142701-95-9; DOPC, 4235-95-4.